Possible regulation of the conventional calpain system by skeletal muscle-specific calpain, p94/calpain 3

Yasuko Ono‡§, Kazumi Kakinuma‡§, Fukuyo Torii‡, Akihiro Irie‡, Kazuhiro Nakagawa‡**, Siegfried Labeit¶, Keiko Abe‡, Koichi Suzuki||***, and Hiroyuki Sorimachi‡§†

‡Department of Applied Biological Chemistry, Graduate School of Agricultural and Life Sciences, University of Tokyo, Tokyo 113-8657, Japan, §CREST, Japan Science and Technology, Kawaguchi 332-0012, Japan, ¶Institut für Anästhesiologie und Operative Intensivmedizin, Universitätsklinikum Mannheim, Germany, ||Tokyo Metropolitan Institute of Gerontology, Tokyo 173-0015, Japan.

†Corresponding author: Laboratory of Biological Function, Department of Applied Biological Chemistry,
Graduate School of Agricultural and Life Sciences, The University of Tokyo,
1-1-1 Yayoi, Bunkyo-ku, Tokyo 113-8657, Japan
TEL/Fax: +81-3-5841-8118, e-mail: ahsori@mail.ecc.u-tokyo.ac.jp

Running Title: Regulation of conventional calpains by p94/calpain 3

SUMMARY

p94 (also called calpain 3) is the skeletal-muscle-specific calpain and is considered to be a "modulator protease" in various cellular processes. Analysis of p94 at the protein level is an urgent issue because the loss of p94 protease activity causes limb-girdle muscular dystrophy type 2A. In this study, we enzymatically characterized one alternatively spliced variant of p94, p94:exons $6^{-}15^{-}16^{-}$ (p94Δ), which lacks two of the p94-specific insertion sequences. In contrast to p94, which has hardly been studied enzymatically due to its rapid, thorough, and apparently Ca^{2+}-independent autolytic activity, p94Δ was stably expressed in COS and insect cells. p94Δ showed Ca^{2+}-dependent caseinolytic and autolytic activities, and an inhibitor spectrum similar to those of the conventional calpains. However, calpastatin did not inhibit p94Δ, and is a substrate for p94Δ, which is consistent with the properties of p94, presenting p94 as a possible regulator of conventional calpain system. We also established a semi-quantitative FRET assay using the calpastatin sequence specifically to measure p94 activity. This method detects the activity of COS-expressed p94 and p94Δ, suggesting that it has potential to evaluate p94 activity *in vivo* and in the diagnosis of LGMD2A.

INTRODUCTION

Calpain (EC 3.4.22.17, clan CA, family C2) is a Ca^{2+}-requiring cysteine protease representing one of the most important families of the cysteine proteases (1-9). To date, various molecules showing significant similarity to the calpain protease domain have been identified in almost all kinds of living organisms and constitute the "calpain superfamily" (6). Two representative members, μ- and m-calpains, the so-called "conventional" calpains, are ubiquitously expressed and have been well characterized. These two calpains consist of a distinct larger catalytic subunit containing a protease domain (μ- or m-calpain large subunit, abbreviated to μCL[1] or mCL, respectively) and a common smaller regulatory subunit (abbreviated to 30K according to its molecular weight). On the basis of amino acid similarities, the large and small subunits have been described as consisting of four and two domains, respectively, which agrees with the recently resolved three-dimensional structure of m-calpain (10, 11; see Fig. 1A).

Conventional calpain has a specific endogenous proteinous inhibitor, calpastatin (12). Calpastatin contains four repetitive inhibitory units, each of which inhibits equimolar amounts of conventional calpain. The conserved reactive site interacts with the calpain protease domain, whereas the flanking α-helical regions bind to domains IV and VI of the large and small subunits, respectively. Synthetic oligopeptides (see Fig. 4D) corresponding to the calpastatin reactive site specifically inhibit conventional calpain efficiently, although their inhibitory activity is weaker

than that of the full-length inhibitory unit.

The primary structure of p94 (also called calpain 3) is very similar to those of μCL and mCL throughout the entire molecule, beyond the p94-specific sequences, NS, IS1, and IS2 (13). Previous studies have revealed several unique characteristics of p94 that diverge greatly from those of the conventional calpains. For instance, [1] p94 undergoes very rapid, thorough, and apparently Ca^{2+}-independent autolysis in solution (half-life *in vitro* is less than 10 min) (14); [2] inhibitors of the conventional calpains, including calpastatin, EDTA, and EGTA, have no effect on p94 autolysis (14); [3] the gene for p94 produces several alternatively spliced products (15, 16); and [4] p94 associates with the N2-line region and the C-terminus of connectin/titin, the gigantic filamentous molecule essential for myofibrils (17, 18; for a review of connectin/titin, see 19-21). The predominant expression of p94 in skeletal muscle, where its mRNA levels are *ca.* 10 times higher than those of μCL and mCL, indicates the physiological importance of p94 in that tissue (13). Consistent with this, a defect in the p94 gene causes limb-girdle muscular dystrophy type 2A (LGMD2A), suggesting that p94 functions are indispensable for proper muscle functions (22). Several studies, including ours, indicate that the loss of substrate-processing activity, but not hyper-activation or a defect in the structural properties of p94, causes LGMD2A (16, 23-26). Therefore, it has become an urgent issue to determine the *in vivo* substrates of p94 to gain insight into the physiological functions of p94 and its relationships

to molecular mechanisms of LGMD2A (27).

However, the autolytic activity of p94 has hampered the study of p94 protein. Therefore, we have focused on identifying the conditions that will allow us to analyse the proteolytic activity of p94. We have previously observed that deletion of either the IS1 or IS2 region, which are mainly encoded by exon 6 or exons 15+16, respectively, prevents the rapid autolysis of p94 (14). In accord with this, we have recently shown that alternatively spliced variants of p94 that lack either exon 6, exons 15+16, or all of these, are detected as non-autolyzed forms, unlike the full-length p94, when they are recombinantly expressed in COS cells (16).

In this study, we chose one of the splicing variants, p94:exons $6^{-}15^{-}16^{-}$ (abbreviated as p94Δ in this paper, see Fig. 1A), which is produced from a transcript lacking exons 6, 15, and 16, and therefore lacks most of the p94-specific insertion sequences, IS1 and IS2, for *in vitro* enzymatic characterization on the basis of its stability and expression efficiency. The enzymatic properties of p94Δ were compared with those of p94, and μ- and m-calpains. We thus identified several novel enzymatic properties of p94. Notably, neither p94 nor p94Δ is inhibited by calpastatin, and moreover, both hydrolyse calpastatin. These results led us to predict that p94 participates in the regulation of the conventional calpain-calpastatin system in skeletal muscle. We used these findings to establish a calpastatin-based fluorescence assay specifically to measure p94 protease activity, showing a possibility to application of this assay to a diagnostic tool for LGMD2A.

EXPERIMENTAL PREOCEDURES

Materials

Enzymes used for manipulating recombinant DNA were purchased from Takara Shuzo Inc. (Kyoto, Japan). The cDNAs for mouse p94/calpain 3 and p94:exons 6$^-$15$^-$16$^-$ (p94Δ) (16), and *Spodoptera frugiperda* cells (Sf-9) were kindly provided by Dr. Muriel Herasse (Généthon, Evry, France), and Dr. Takeshi Nishino (Nippon Medical School, Tokyo, Japan), respectively. A baculovirus expression vector, pFastBac1, culture media, and transfection reagent were purchased from Invitrogen Inc. (CA, USA). Mammalian expression vectors, pECFP-N1 and pEYFP-N1, were purchased from BD Biosciences Clontech Inc. (CA, USA). Casein was purchased from Merck (Frankfurt, Germany). Protease inhibitors were purchased from Calbiochem Inc. (CA, USA), Peptide Institute Inc. (Osaka, Japan), or Sigma Inc. (MO, USA). Other chemicals were obtained from Nacalai Tesque Inc. (Kyoto, Japan), or Wako Pure Chemicals (Osaka, Japan).

p94-specific anti-pNS (antigen: PTVISPTVAPRTGAEPRS at the N-terminus) and anti-pIS2 (identical to anti-pK-rich, antigen: NTISVDRPVKKKKNKPIIFV overlapping with the IS2 region) antisera have been described previously (14). Monoclonal antibodies 2C4 and 12A2, which recognize N-terminus and the region around the catalytic residue Asn358 of p94, respectively, were purchased from Novacastra Laboratories Ltd. (Newcastle, UK). Monclonal

antibodies which recognize μCL and mCL were purchased from Biomol Research Laboratories Inc. (PA, USA) and Chemicon International Inc. (CA, USA), respectively. Recombinant domain 1 of human calpastatin protein and the peptides corresponding to its reactive site were purchased from Takara Shuzo Inc. (7316 and SP007) and Sigma Inc. (C9181).

Recombinant proteins expressed in insect cells

The cDNA for p94Δ or p94:C129S, an active-site mutant, was inserted into the pFastBac1 vector using appropriate restriction enzyme sites. Recombinant baculovirus was generated according to the manufacturer's instructions. Sf-9 cells were cultured and infected as previously described (28). The cells were then shaken vigorously at 27 °C for 50 h at a density of 1×10^6 cells/ml, and collected by centrifugation at 600 × g for 5 min at 4 °C. Recombinant proteins were purified following the procedures described previously (28), with minor modifications as follows. The harvested cells were washed twice with ice-cold phosphate-buffered saline (PBS). The pellets were suspended in buffer A (20 mM Tris-Cl [pH 7.5], 5 mM EDTA, 10 mM 2-mercaptoethanol [2-ME]) containing 0.1 mM leupeptin, and the cells were homogenized with a French press (American Instrument Co., MD, USA). The cell lysate was then ultracentrifuged at 150,000 × g for 40 min at 2 °C. Recombinant proteins were purified from the supernatant by the AKTA system (Amersham Biosciences Inc., Amersham, UK) placed in a cold chamber, using

successive rounds of column chromatography: DEAE-Toyopearl (Tosoh Inc., Tokyo, Japan), MonoQ (Amersham Biosciences Inc.), HiLoad 16/60 Superdex200, and MonoQ. Fractions containing recombinant proteins were determined by western blotting analysis and caseinolytic assays (for p94Δ). Recombinant μ- and m-calpains were prepared in the manner described in ref 28.

Bacterial expression and purification of recombinant proteins

cDNA fragments corresponding to two different N2A regions of connectin/titin, IgI80-81 and IgI82-83, were amplified by PCR from human skeletal muscle cDNA and cloned into the pET vector. Proteins were expressed in *E. coli.* BL21(DE3) and purified as previously described (29).

A bacterial expression vector for the fusion protein generated from enhanced cyan and yellow fluorescence proteins (ECFP and EYFP, respectively) linked by a part of rabbit calpastatin domain 1 (residues 175-255, GenBank accession number A26615), Y-C-CSTN, was created by fusing the PCR-amplified coding sequences of ECFP, EYFP, and calpastatin, and cloning the construct into the pET16b vector. The recombinant protein, Y-C-CSTN, expressed in *E. coli.* BL21(DE3), was purified by His-Bind Quick 900 Cartridges (Novagen, WI, USA), according to the manufacturer's protocol. Protein fractions eluted from the cartridge were desalted on a

PD-10 column (Amersham Biosciences Inc.) and concentrated by Centricon (Millipore, MA, USA).

Protease activity assay

Caseinolytic activity of p94Δ was measured essentially according to ref 30. In brief, the composition of the standard assay solution was 100 mM Tris-Cl (pH7.5), 25 mM 2-ME, 10 mM $CaCl_2$. $CaCl_2$ was replaced with 10 mM EDTA for the control reaction. The reaction was carried out by incubating either p94Δ (3 μg), μ-calpain (0.2 μg), or m-calpain (0.4 μg) in 50 μl of the standard assay solution containing 3 mg/ml casein under the conditions indicated. The reaction was stopped by the addition of 150 μl of 7% (w/v) trichloroacetic acid. The tubes were incubated on ice for 20 min, centrifuged at 15,000 × g for 10 min, and the A_{280} of the supernatant measured. An increase in A_{280} of 1.0 in 1 h was defined as 1 unit of caseinolytic activity. The effect of Ca^{2+} on p94Δ was determined under the assay conditions described above, varying either the concentration of Ca^{2+}, temperature, or pH. Tris-acetate buffer was used instead of Tris-Cl buffer to measure the effect of pH. Protease inhibitors were added to the standard assay solutions at the concentrations indicated. The reactions were carried out at 37 °C for 45 min and the caseinolytic activity was determined as described. The effect of each inhibitor was evaluated relative to the inhibitory effect of 10 mM EDTA set to 100.

To determine the substrate-hydrolysing activity of p94Δ, various proteins were incubated with p94Δ in the standard assay solution. Hydrolysis of the proteins was examined by sodium dodecyl sulfate-polyacrylamide gel electrophoresis (SDS-PAGE) followed by Coomassie Brilliant Blue (CBB) staining or western blotting.

In the proteolytic assay using Y-C-CSTN as substrate, 2 μg of Y-C-CSTN was incubated with p94Δ in the presence of 15 mM Ca^{2+} for 0-45 min at 37 °C in a solution containing 0.1 M Tris-Cl (pH 7.5) and 10 mM 2-ME in a volume of less than 20 μl. The reaction was stopped by the addition of 0.5 ml of 0.1 M EDTA (pH 8.0) or an equal volume of 2 × SDS sample buffer. The fluorescence of the samples was measured by excitation at 434 nm (10 nm bandwidth), and the emission spectra were collected from 450 to 600 nm using an RF-1500 spectrofluorophotometer (Shimazu Inc., Kyoto, Japan). The ratio of fluorescence at 477 nm to that at 527 nm was used to define proteolytic activity. To profile the dose-dependent changes in fluorescent signals, 0-2 μg of p94Δ was incubated with Y-C-CSTN (0.6 μg) in a buffer consisting of 28 mM Ca^{2+}, 1 mg/ml bovine serum albumin (BSA), 0.1 mg/ml calpastatin (CSTN) domain 1, 20 mM 2-ME, and 100 mM Tris-Cl (pH 7.5) in a total volume of 15 μl for 5-45 min.

Cell culture and assays

COS-7 cells were maintained and transfected with each plasmid construct as described previously

(24). The cell lysate was prepared by sonicating harvested cells in a solution consisting of 50 mM Tris-Cl (pH 7.5), 25 mM 2-ME, 10 mM EDTA, and the proteinase inhibitors 10 μM Z-D-CH2-DCB, 10 μM YVAD-CMK, 1 mM AEBSF, 2 μM calpastatin peptide C9181, and 2 mM phenylmethylsulfonyl fluoride (PMSF).

To detect p94 activity in the cell lysate, the following protease inhibitors were added to the standard assay mixture described above to inhibit the conventional calpains and other proteases: 10 μM Z-D-CH2-DCB, 10 μM YVAD-CMK, 1 mM AEBSF, 2 μM calpastatin peptide C9181, and 2 mM PMSF. The same number of COS-7 cells (2-3 × 10^5) transfected with each plasmid were incubated with Y-C-CSTN in the presence of 5 mM Ca^{2+} or 10 mM EDTA in total volume of 20 μl for 90 min at 37 °C, after which 0.5 ml of 0.1 M EDTA was added. To detect the autolysis of p94 and p94Δ by western blotting, the reaction was stopped by the addition of half a volume of 3 × SDS sample buffer.

Other protein experiments

SDS-PAGE, western blotting, and subsequent procedures were performed as previously described (14). Proteins were transferred onto polyvinylidene difluoride membranes (Immobilon-P, Millipore Inc.), as recommended by the supplier, and incubated with specific antisera as indicated. The secondary antibody was horseradish peroxidase-coupled goat anti-rabbit or goat anti-mouse

IgG (Nichirei Inc., Tokyo, Japan). The antibody complexes were visualized using peroxidase substrate (POD Immunostaining Kit; Wako Inc., Osaka, Japan). To examine the autolytic activity of p94Δ, 1 μg of p94Δ was incubated in 15 μl of solution containing 100 mM Tris-Cl (pH 7.5), 25 mM 2-ME, and 10 mM $CaCl_2$, at either 0 °C or 30 °C for the indicated times. The reaction was stopped by the addition of an equal volume of 2 × SDS sample buffer and subjected to SDS-PAGE followed by CBB staining or western blotting, as described above.

Protein concentrations were measured using a DC Protein Assay Kit (Bio-Rad Inc. CA, USA) with BSA as the standard. The N-terminal amino acid sequence of the protein fragments was determined on an Applied Biosystems protein sequencer type 477A/120A, according to manufacturer's instructions and the method described previously (31), with some modification.

RESULTS

Expression and purification of p94Δ and p94:C129S

Recombinantly expressed p94Δ and p94:C129S (a protease-inactive point mutant of p94/calpain 3) were purified by four successive rounds of column chromatography, as described in Materials and Methods (see Fig. 1A for structures of p94Δ and p94:C129S). The purity of these products was estimated to be more than 90% based on a CBB-stained gel after SDS-PAGE, as shown in Fig. 1B. The N-terminal sequence of purified p94Δ revealed that, after two weeks storage at 2 °C, most of the purified p94Δ had been hydrolysed on the N-terminus of Ala34 (Fig. 1A, arrow [4]), and that anti-pNS antiserum, raised against a peptide corresponding to N-terminal residues 2-19 (14), no longer recognized the purified protein. The p94Δ sample was recognized by anti-pNS antiserum just after purification. p94:C129S, which was purified by a procedure identical to that used for p94Δ, showed no hydrolysis at the N-terminus. Therefore, we concluded that the hydrolysis of p94Δ was autolytic. This autolysis occurred in the presence of 5 mM EDTA, even at 2 °C, which is consistent with our previous observation that p94 rapidly undergoes autolysis in the presence of excess EDTA (14).

The yields of totally purified p94Δ and p94:C129S proteins were *ca.* 1.2 and 2.4 mg/l culture, respectively. Although the N-terminal autolysis of p94Δ did not require Ca^{2+}, p94Δ showed Ca^{2+}-dependent caseinolytic activity (see Fig. 2; details are discussed later). Analysis of the

degraded casein by SDS-PAGE indicated that p94Δ degrades casein in a manner similar to the caseinolysis by the conventional calpains (data not shown). The specific activity of p94Δ determined by caseinolysis was 9.0 unit/mg, which is *ca.* 1/80 of the value for recombinant human m-calpain determined with the same expression and purification systems (28, 32, 33). However, because most of the purified p94Δ underwent N-terminal autolysis as described above, we concluded that very low specific caseinolytic activity is one of the enzymatic properties of p94Δ, and does not result from partial denaturation or aggregation of the protein.

Enzymatic properties of p94Δ: effects of temperature, pH, Ca^{2+}-concentration, and protease inhibitors

The caseinolytic activity of p94Δ was examined while varying either temperature, pH, or Ca^{2+}-concentration, and compared with the corresponding parameters for recombinant μ- and m-calpains. Fig. 2A shows the temperature-dependence of p94Δ caseinolytic activity. The initial rate of p94Δ activity increased with temperature. In the range of temperatures examined here, the activity of p94Δ increased persistently with time up to 60 min. The optimal temperature for 20 min incubation of p94Δ was about 42 °C, which contrasts with the decrease in activity observed for both μ- and m-calpains at temperatures above 25 °C (Fig. 2B). Although p94Δ shows maximum activity at around pH 7.5, as do other calpains, p94Δ maintains its activity

even at pH 10 (Fig. 2C). Ca^{2+}-dependence showed that a pCa for half maximal activity for p94Δ was 2.9, which is lower than those of μ- and m-calpains (3.7 and 3.3, respectively) (Fig. 2D).

The effects of various inhibitors on the activity of p94Δ and μ- and m-calpains were investigated (Table 1). p94Δ has a spectrum of inhibitors very similar to those of μ- and m-calpains, except calpastatin. The calpastatin fragment inhibited μ- and m-calpains completely at molar ratios of almost 1:1, whereas p94Δ was not inhibited by a 100-fold molar excess of the calpastatin fragment or calpastatin-related peptides (Fig. 2E). In fact, calpastatin was shown to be a substrate for p94Δ (see below). Because the IS1 region is a target for p94 autolysis (31, 34), we examined the possibility that synthetic peptides corresponding to IS1 would have a competitive inhibitory effect on p94. However, none of the peptides inhibited the caseinolytic activity of p94Δ, even at a molar ratio of 100:1 (data not shown).

Autolytic activity of p94Δ

p94Δ is much more stable than full-length wild-type p94. However, as described above, limited autolysis at the N-terminus of p94Δ occurs even in the presence of EDTA at 2 °C. Therefore, the autolytic activity of p94Δ was analysed in more detail. p94Δ, already lacking the N-terminal 33 amino acids of p94, underwent further autolysis in the presence of Ca^{2+}. As shown in Figs.

2F and 2G, this second-phase autolysis generated an 83-kDa fragment very rapidly ($t_{1/2}$ = 5 min at 30 °C, and 20 min at 0 °C). No change in caseinolytic activity or Ca^{2+}-dependence was caused by preincubation of p94Δ for 5, 10, 20, or 60 min at 30 °C (data not shown). The N-terminal sequence of the 83-kDa fragment was also from Ala34, indicating that the second autolysis occurs at the C-terminus of p94Δ (data not shown).

To characterize further the autolytic activity of p94Δ relative to that of full-length wild-type p94, p94:C129S, a good "intermolecular autolytic" substrate for p94, was proteolysed by p94Δ (24). Co-incubation of p94:C129S (1 μg) and p94Δ (0.1 μg) resulted in the production of four major fragments with approximate molecular weights of 93 kDa, 91 kDa, 58 kDa, and 33 kDa, as shown in Fig. 2H. Interestingly, none of these fragments was recognized by anti-pNS antiserum, and the full-length 94-kDa protein detected by anti-pNS antiserum decreased rapidly in the reaction. The N-terminal residue of the 93-kDa fragment (Fig. 2H, (a)) was Ala15 (Fig. 1A, arrow [1]), whereas the N-terminal residues of the 91-kDa and 33-kDa fragments (Fig. 2H, (b) and (d), respectively) were identical to that of N-terminally autolyzed p94Δ (Ala34, Fig. 1A [2]). These results indicate that p94Δ very efficiently hydrolyses the N-terminus of p94:C129S, as well as that of p94Δ itself. The N-terminal residue of the 58-kDa fragment (Fig. 2H, (c)) was Glu323 (Fig. 1A [3]), which corresponds to one of the previously determined autolytic sites in native p94 (31). The 33-kDa fragment was not detected by either the monoclonal antibody 12A2 or

anti-pIS2 antiserum. These results indicate that p94:C129S is hydrolysed by p94Δ first at the N-terminus and then in the region of IS1, which generates 58-kDa and 33-kDa fragments corresponding to the C- and N-terminal parts of the 91-kDa fragment, respectively.

Substrates for p94Δ

Previously, we found that p94 causes a decrease in a 60-kDa protein *in vivo*, when expressed in COS cells (14). Peptide sequencing revealed that it corresponds to heat shock protein 60 (HSP60). Consistent with this, an *in vitro* assay showed that p94Δ proteolyses HSP60 (Fig. 3A). Moreover, HSP60 is proteolysed by m-calpain much more rapidly than by p94Δ, suggesting that HSP60 is also a possible *in vivo* target of the conventional calpains. Although HSP60 is highly conserved from bacteria to eukaryotes (*ca.* 50% primary sequence identity between human and *Escherichia coli* proteins), the *E. coli* HSP60 homologue, GroEL, is very poorly hydrolysed by p94Δ. Its co-chaperonin, GroES, and combinations of GroEL and ES with or without ATP were also examined, but none was proteolysed by p94Δ (data not shown).

Several other proteins were incubated with p94Δ to test whether they are substrates. Two different N2A fragments of connectin/titin, IgI80-81 and IgI82-83, were hydrolysed by p94Δ as well as μ- and m-calpains. The connectin constructs IgI80-81 and IgI82-83 contain the two N-terminal and the two C-terminal Ig motifs of the N2A region, respectively. IgI82-83 includes

a p94-binding site for connectin (Fig. 3B) (17). IgI80-81 was more rapidly degraded than IgI82-83 by p94Δ and μ- and m-calpains, as shown in Fig. 3C. N-terminal sequencing of the degradation fragments of IgI80-81 revealed that one of the proteolytic sites susceptible to calpain is on the N-terminus of Gly9434 (GenBank accession number NP_596869; ref 35; Fig. 3B, arrow) in I80. These results strongly suggest that not only μ- and m-calpains but also p94 proteolytically degrade connectin/titin.

Protease-inactive m-calpain, m-calpain:C105S, was proteolysed by p94Δ, as shown in Fig. 3D, whereas p94:C129S was not hydrolysed by m-calpain (data not shown). It should be mentioned that anti-pIS2 detects p94Δ since a part of the epitope is retained in p94Δ. Notably, the addition of the calpastatin domain 1 fragment (Fig. 3D, +CSTN) abolished m-calpainolysis by p94Δ, but not autolysis of p94Δ or caseinolysis by p94Δ (Fig. 2E), suggesting that the m-calpain-calpastatin complex acquires resistance to proteolysis by p94Δ in the presence of Ca^{2+}. A widely used fluorescent substrate for the conventional calpains, Suc-LLVY-MCA, was not significantly hydrolysed by p94Δ (data not shown).

These results show that some of the substrates for p94Δ (and for p94) can be hydrolysed by the conventional calpains as well (casein, HSP60, connectin/titin N2A fragments, and m-calpain:C105S). On the contrary, calpastatin and p94:C129S are hydrolysed more efficiently and exclusively, respectively, by p94Δ and p94.

Proteolysis of calpastatin by p94Δ

Proteolysis of the calpastatin domain 1 fragment (14.1 kDa, residues 27-159 of human calpastatin, GenBank accession number NP_775085; Takara Shuzo Inc. No. 7316) by p94Δ was examined by reversed-phase column chromatography. The calpastatin fragment was rapidly degraded proteolytically by p94Δ into several fragments, as shown in Figs. 4A and 4B, and the N-terminal sequences were determined. Six cleavage sites were identified (Fig. 4C, lines i-vi; four of these are shown in Fig. 4D), one of which is located close to the reactive site (i). The others (ii-vi), if cleaved, result in the loss of one of the helical regions on the C-terminal side of the reactive site, which interacts with domain VI of the conventional calpains. All six cleavage sites are different from the cleavage sites of the caspases (Fig. 4D, open triangle; 36). These results indicate that the cleavage of calpastatin by p94 inactivates the calpain-inhibitory activity of calpastatin. The most susceptible sites are on the N-terminus of Ala105 and Gly124 (accession number NP_775085; ii and iv in Figs. 4C and 4D), which are detectable in the fractions already appearing after 20 min digestion (Fig. 4A, closed triangles). These sites both have Pro at the P3' position and a small amino acid (Ala and Gly) at the P1' position. Moreover, five out of six cleavage sites in the calpastatin domain 1 fragment have two Pro residues between P2' and P8'. These features may reflect the proteolytic preference of p94. One of the autolytic sites in p94:C129S

and p94Δ, the N-terminus of Ala15, also has Pro at the P3' position and a small amino acid (Ala) at the P1' position (Fig. 4C, N-1). However, there are no further significant similarities found between the amino acid sequences surrounding the cleavage sites in calpastatin and those for autolytic sites in p94:C129S and p94Δ (Fig. 4C, N-2 and IS1-1~3) (31).

To test whether p94Δ proteolytically degrades short peptides, a 27-mer peptide corresponding to the reactive site of calpastatin (Sigma C9181; Fig. 4D) was incubated with p94Δ. Although the efficiency of cleavage was very low (less than 5% after 120 min incubation), the peptide was cleaved on the N-terminus of Lys99 (Figs. 4C and 4D, vii). The site has Pro residues at the P1 and P2 positions but not in the P' positions, suggesting that short peptides are cleaved by p94Δ differently from the cleavage of calpastatin domain 1 fragment, which is a much better substrate for p94Δ.

Assay system for p94 utilizing calpastatin as substrate

As observed above, calpastatin is the best substrate for p94Δ among the protein substrates examined in this study except for p94:C129S. Therefore, we developed an assay for p94 using the calpastatin fragment and fluorescent resonance energy transfer (FRET). When the purified substrate, Y-C-CSTN (Fig. 5A), was incubated with p94Δ, it was rapidly degraded into several fragments (Fig. 5B). Before the substrate was cleaved by p94Δ, the fluorescence spectrum of

Y-C-CSTN excited at 434 nm, the CFP excitation wave length, showed a peak at 527 nm, which is an emission wavelength of YFP, indicating that YFP is excited by the CFP emission by FRET (Fig. 5C, 0 min). The emission spectrum of Y-C-CSTN excited at 434 nm was measured during the proteolytic process. A time-dependent increase in CFP emission at 477 nm and a corresponding decrease in YFP emission at 527 nm was observed, demonstrating that the proteolysis of Y-C-CSTN by p94Δ can be monitored as the change in the emission spectrum caused by the loss of FRET between those two fluorescent units (Fig. 5C). Various amounts of p94Δ were tested for Y-C-CSTN digestion and the ratio of YFP emission to CFP emission, 477 nm/527 nm, was plotted for each time point (Fig. 5D). The increase in the fluorescence ratio 477/527 was time- and dose-dependent, and the activity of as little as 250 ng of p94Δ could be assayed with an incubation of 45 min. μ-calpain produced no increase in the fluorescence ratio nor proteolysis of Y-C-CSTN over this period of time or in this range of protein concentrations (data not shown), suggesting that Y-C-CSTN is a p94Δ-specific substrate but not for the conventional calpains under our assay condition.

Activity of COS-expressed full-length wild-type p94 detected by Y-C-CSTN

To test whether the assay described above can detect the proteolytic activity of full-length wild-type p94, as well as the activity of p94Δ, among one hundred other co-occurring proteases

in vivo, the proteolytic activity of p94 expressed in COS7 cells was measured using Y-C-CSTN as substrate. COS cells are known to express considerable amounts of m-calpain and other cellular proteases, such as caspases. Ca^{2+}-dependent proteolysis of Y-C-CSTN was detected in the lysates of cells expressing full-length wild-type p94 (Fig. 5E, f.l.p94) or p94Δ (Fig. 5E, p94Δ) in the presence of protease inhibitors for major proteases including conventional calpains, caspases, and serine proteases. On the other hand, the lysates of cells expressing protease-inactive full-length p94:C129S (Fig. 5E, CS) or μ-calpain (Fig. 5E, μ-calpain) showed no activity above background levels, *i.e.*, above the value determined for cells transfected with empty vector, regardless of enough amount of the proteins detected (Fig. 5F, CS and μ-calpain). These results clearly indicate that our assay system specifically detects and distinguishes the protease activity of p94 in the presence of interfering proteases.

To our surprise, full-length wild-type p94 showed Ca^{2+}-dependent calpastatinolytic activity (Fig. 5E, f.l.p94). The autolysis of recombinantly expressed p94, however, was Ca^{2+}-independent (Fig. 5F, f.l.p94; grey arrow head) as shown previously (14), which is consistent with the fact that most COS-expressed p94 had already disappeared at harvest. These results indicate that the autolysis of p94 does not require Ca^{2+}, whereas calpastatinolysis occurs in a Ca^{2+}-dependent manner, suggesting different substrate specificities for p94 in the absence and presence of Ca^{2+}.

DISCUSSION

In this study, the enzymatic properties of one of the alternatively spliced variants of p94/calpain 3 were examined, to understand better the unique characteristics of p94 and their relevance to its physiological functions. Isolating significant amounts of the proteins is a prerequisite for *in vitro* enzymatic studies, and this has been almost impossible owing to the very rapid autolytic activity of p94 (31). On the other hand, some natural splice variants of p94 expressed in skeletal muscle are somewhat stable. After several different isoforms were examined, p94Δ, which lacks both IS1 and IS2, was the most promising variant for large-scale preparation. The structure of p94Δ is almost identical to that of μCL and mCL, except that it has the NS. It shows proteolytic characteristics similar to those of μ- and m-calpains, such as Ca^{2+}-dependence, insofar as IS1 and IS2 are involved in Ca^{2+}-independent protease and autolytic activity, a hallmark of p94.

However, there are several traits distinguishing p94Δ from the conventional calpains: (1) p94Δ shows specific caseinolytic activity much lower than those of the conventional calpains, (2) the optimal temperature for p94Δ activity is higher (*ca.* 42°C) than those of the conventional calpains (25-30°C), and (3) p94Δ has a lower pCa for half maximal activity than μ- or m-calpains. At present, the possibility cannot be excluded that these properties originate from the lack of IS1 or IS2. It should be emphasized, however, that many features of p94Δ are shared with full-length

p94: neither is inhibited by, but proteolytically degrades calpastatin; both exhibit proteolytic activity without 30K; both bind connectin/titin at the N2A and M-line regions (16); both cut p94:C129S at identical sites; and both undergo autolysis in the presence of EDTA. Therefore, it is conceivable that the properties of p94Δ described above reflect the nature of p94 and are related to the functions of p94 in the context of the physiology of skeletal muscle.

Stable and active without 30K

The co-expression of 30K is required for recombinant μ- and m-calpains and nCL-4 in the same Sf-9/baculovirus system (28, 32, 33, 37, 38). However, proteolytically active p94Δ and inactive p94:C129S were isolated in the soluble and stable fraction without 30K. Furthermore, no interaction between p94Δ and 30K was detected in the yeast two-hybrid system, as was also the case for p94 (17, 16). These data strongly suggest that p94Δ and p94 do not form heterodimers with 30K. It awaits further analyses on the tertiary structures of p94Δ and p94 to determine if they form homodimers which was predicted from the elution positions of p94:C129S and p94Δ on the gel-filtration column (31 and data not shown).

Autolytic activity of p94 and p94Δ

Our previous results on the *in vitro* translation of p94 indicated that the autolysis of p94 proceeds

in the presence of excess EDTA (14), which was also observed for the N-terminal autolysis of p94Δ. Branca *et al.*, however, reported Ca^{2+}-dependent proteolytic fragmentation of recombinant p94 (39). They isolated a substantial amount of full-length wild-type p94 using the Sf-9/baculo virus system. In our hands, however, p94:C129S was expressed abundantly and stably, and was successfully purified almost to homogeneity using the same Sf-9/baculo virus system (Fig. 1B), whereas wild-type p94 expressed in the same system was detected only as a 55-kDa autolyzed fragment (data not shown). At present, no clear explanation is available for these discrepancies, but p94 may show Ca^{2+}-dependent autolysis under certain conditions. Indeed, Ca^{2+}-dependent hydrolytic activity was detected for full-length wild-type p94 as well as for p94Δ using a calpastatin-based FRET substrate in this study.

Hydrolysis of p94:C129S by p94Δ, but not by m-calpain, strongly suggests that the substrate specificities of p94Δ and p94 are the same. In addition to the autolytic site in IS1 (31), p94Δ hydrolyses p94:C129S at the N-termini of Ala15 and Ala34. In this study, one of the intramolecular autolytic sites of p94Δ was also demonstrated to be Ala34. Ca^{2+}-independent autolysis at the N-terminus of Ala34 generates a rather stable autolytic fragment of p94Δ since no further autolysis occurred during the storage of p94Δ for over a year (data not shown). Recently, Rey and Davies reported that one of the autolytic sites in a recombinant protein corresponding to the protease domain of p94 was Ala15 (34), which is consistent with our result. They also

reported Ala45 and Thr316 as autolytic sites, which were not identified in our experiments. It can be reasoned that the lack of domain III and regions thereafter in their construct exposed sites potentially susceptible to autolytic cleavage. Previously, we have observed that the Ca^{2+}-independent autolytic activity of recombinant p94:exon6$^-$ was much weaker than that of full-length p94, resulting in the stabilization of p94:exon6$^-$ (16 and unpublished data). Therefore, it is inferred that the lack of exon 6, which constitutes most of IS1, contributes to the stability of p94Δ by abrogating the pivotal autolytic site. Rey and Davies also reported Ca^{2+}-dependent autolysis of their protein, which can be ascribed to the lack of IS2 based on our previous observations (16 and unpublished data). Very recently, Fukiage *et al.* reported the qualitative characterization of Lp82 (40), another alternative splice variant of p94, which is specifically expressed in the lens. They showed that the lack of IS2 does not effectively stabilize the product when NS is replaced by AX1, a lens-specific N-terminal sequence (41). Considering these data together, we conclude that NS, IS1, IS2, and AX1, unique sequences specific to *CAPN3* proteins, have independent functions, and that different combinations of them confer specific characters, *e.g.*, different autolytic activities, upon each splice variant.

p94-specific assay towards a diagnosis of LGMD2A

Because the loss of the substrate-processing activity of p94 causes LGMD2A (24), we have

focused on identifying its substrates. One of the major problems we faced was how to distinguish the activity of p94 from that of other proteases, including the conventional calpains, in a physiological context. The enzymatic properties determined for p94Δ in this study showed that there are conditions favourable for p94 but not for the conventional calpains, such as high temperature and the presence of calpastatin. Consequently, we established a specific assay system for p94 and demonstrated its ability to identify COS-7-expressed p94, as well as p94Δ. In theory, 0.3 mg muscle, which corresponds to about three 10 μm cryostat slices of a muscle biopsy, contains at least 300 ng of p94 (42). Our system can assay as little as 250 ng of p94Δ. The activity of the COS-7-expressed p94 and p94Δ detected in this study corresponds to a minimum of approximately 10 ng of protein. Therefore, we anticipate that the activity of endogenous p94 in tissues (biopsy samples) will be measurable using this assay, and that this methodology will be applicable to the diagnosis of LGMD2A by screening for the loss of p94 activity.

Calpain network and LGMD2A

The apparently Ca^{2+}-independent proteolysis of p94:C129S and calpastatin is p94-specific, which is not observed for the conventional calpains (17). m-calpain:C105S was also degraded proteolytically by p94Δ in a Ca^{2+}-dependent manner, although p94:C129S was not degraded by

m-calpain. These results imply, for the first time, that p94 has a certain role in regulating the conventional calpains directly and indirectly by proteolytic degradation of the calpains and calpastatin, respectively.

It has been reported that there are several biological context where several different protease systems keep cross-talking. For example, calpain and caspase proteolytic systems function synergically in apoptosis, where proteolytic inactivation of calpastatin by caspase facilitates calpain activation and calpain activates caspase by limited proteolysis (43). It has not yet been, however, shown whether there is a cross-talk between p94 and the conventional calpains, the so-called "calpain network" in skeletal muscle where the expression level of p94 predominates. It is already clear that the function of p94 cannot be completely compensated by other calpains since a defect of p94 function causes LGMD2A. It is, therefore, of our interest to investigate mechanisms how p94 could intervene in the conventional calpain system, which would be compromised in LGMD2A.

ACKNOWLEDGEMENTS

We are very grateful to Dr. Muriel Herasse (Généthon, Evry, France), Dr. Takeshi Nishino (Nippon Medical School, Tokyo, Japan), and Dr Hajime Masumoto (Toray Inc., Kanagawa, Japan) for providing us with mouse cDNAs for p94 and its variants, Sf-9 cells, and recombinant μ- and m-calpains, respectively. We would also like to thank Prof Shoichi Ishiura, Dr Tatsuya Maeda, Dr Ichiro Matsumoto, and Dr Akihito Yasuoka of the University of Tokyo, Dr Hiroyuki Kawahara of the University of Hokkaido, Dr Takaomi C. Saido of the Riken Institute, Dr Noriko Sorimachi of Tokyo Medical and Dental University, and all the other "Team Calpain" members (Dr Shoji Hata, Dr Eiichi Kimura, Ms Yukiko Kawabata, Mr Katsuhide Yoshioka, Mr Suguru Koyama, and Mr Yoshitaka Yamamuro) of the Graduate School of Agricultural and Life Sciences in the University of Tokyo, for their generous gifts of experimental materials, valuable discussions, and encouragement. This work was supported in part by a Grant-in-Aid for Scientific Research on Priority Areas (Cell Cycle) from the Ministry of Education, Science, Sports and Culture, a Grant-in-Aid for Scientific Research and Research Fellowships for Young Scientists from JSPS (the Japan Society for the Promotion of Science), a Research Grant (14B-4) for Nervous and Mental Disorders from the Ministry of Health, Labour and Welfare, the Deutsch Forschungsgemeinschaft (La668/7-1), and "Ground-based Research Announcement for Space Utilization" promoted by the Japan Space Forum.

REFERENCES

1. Sorimachi, H., Ishiura, S. and Suzuki, K. (1997) *Biochem. J.* **328**, 721-732

2. Carafoli, E. and Morinari, M. (1998) *Biochem. Biophys. Res. Commmun.* **247**, 193-203

3. Ono, Y., Sorimachi, H. and Suzuki, K. (1998) *Biochem. Biophys. Res. Commun.* **245**, 289-294

4. Tidball, J. G.. and Spencer, M. J. (2000) *Int. J. Biochem. Cell Biol.* **32**, 1-5

5. Huang, Y. and Wang, K. K. (2001) *Trends Mol. Med.* **7**, 355-362

6. Sorimachi, H. and Suzuki, K. (2001) *J. Biochem.* **129**, 653-664

7. Glading, A., Lauffenburger, D. A. and Wells, A. (2002) *Trends Cell Biol.* **12**, 46-54

8. Jia, Z., Hosfield, C. M., Davies, P. L. and Elce, J. S. (2002) *Methods Mol. Biol.* **172**, 51-67

9. Perrin, B. J. and Huttenlocher, A. (2002) Calpain. *Int. J. Biochem. Cell Biol.* **34**, 722-725

10. Hosfield, M. C., Else, S. J., Davies, L. P. and Jia, Z. (1999) *EMBO J.* **18**, 6680-6889

11. Strobl, S., Fernandez-Catalan, C., Braun, M., Huber, R., Masumoto, H., Nakagawa, K., Irie, A., Sorimachi, H., Bourenkow, G., Bartunik, H., Suzuki, K. and Bode, W. (2000) *Proc. Natl. Acad. Sci. USA* **97**, 588-592

12. Todd B, Moore D, Deivanayagam CC, Lin G, Chattopadhyay D, Maki M, Wang KK, Narayana SV. (2003) *J. Mol. Biol.* **328**, 131-146

13. Sorimachi, H., Imajoh-Ohmi, S., Emori, Y., Kawasaki, H., Ohno, S., Minami, Y. and

Suzuki, K. (1989) *J. Biol. Chem.* **264**, 20106-20111

14. Sorimachi, H., Toyama-Sorimachi, N., Saido, T. C., Kawasaki, H., Sugita, H., Miyasaka, M., Arahata, K., Ishiura, S. and Suzuki, K. (1993) *J. Biol. Chem.* **268**, 10593-10605

15. Ma, H., Fukiage, C., Azuma, M. and Shearer, T. R. (1998) *Invest. Ophthalmol. Vis. Sci.* **39**, 454-461

16. Herasse, M., Ono, Y., Fougerousse, F., Kimura, E., Stockholm, D., Beley, C., Montarras, D., Pinset, C., Sorimachi, H., Suzuki, K., Beckmann, J. S. and Richard, I. (1999) *Mol. Cell. Biol.* **19**, 4047-4055

17. Sorimachi, H., Kinbara, K., Kimura, S., Takahashi, M., Ishiura, S., Sasagawa, N., Sorimachi, N., Shimada, H., Tagawa, K., Maruyama, K. and Suzuki, K. (1995) *J. Biol. Chem.* **270**, 31158-31162

18. Kinbara, K., Sorimachi, H., Ishiura, S. and Suzuki, K. (1997) *Arch. Biochem. Biophys.* **342**, 99-107

19. Gregorio, C. C., Granzier, H., Sorimachi, H. and Labeit, S. (1999) *Curr. Opin. Cell Biol.* **11**, 18-25

20. Trinick, J. and Tskhovrebova, L. (1999) *Trends Cell Biol.* **9**, 377-380

21. Maruyama, K. (2002) *Trends Biochem. Sci.* **27**, 264-266

22. Richard, I., Broux, O., Allamand, V., Fougerousse, F., Chiannilkulchai, N., Bourg, N.,

Brenguier, L., Devaud, C., Pasturaud, P., Roudaut, C., Hillaire, D., Passos-Bueno, M.-R., Zatz, M., Tischfield, J. A., Fardeau, M., Jackson, C. E., Cohen, D. and Beckmann, J. S. (1995) *Cell* **81**, 27-40

23. Richard, I., Roudaut, C., Marchand, S., Baghdiguian, S., Herasse, M., Stockholm, D., Ono, Y., Suel, L., Bourg, N., Sorimachi, H., Lefranc, G., Fardeau, M., Sébille, A., and Beckmann, J. S. (2000) *J. Cell. Biol.* **151**, 1583-1590

24. Ono, Y., Shimada, H., Sorimachi, H., Richard, I., Saido, T. C., Beckmann, J. S., Ishiura, S. and Suzuki, K. (1998) *J. Biol. Chem.* **273**, 17073-17078

25. Spencer, M. J., Guyon, J. R., Sorimachi, H., Potts, A., Richard, I., Herasse, M., Chamberlain, J., Dalkilic, I., Kunkel, L. M. and Beckmann, J. S. (2002) *Proc. Natl. Acad. Sci. U.S.A.* **99**, 8874-8879

26. Tagawa, K., Taya, C., Hayashi, Y. K., Nakagawa, M., Ono, Y., Fukuda, R., Karasuyama, H., Toyama-Sorimachi, N., Katsui, Y., Hata, S., Ishiura, S., Nonaka, I., Seyama, Y., Arahata, K., Yonekawa, H., Sorimachi, H. and Suzuki, K. (2000) *Hum. Molec. Genet.* **9**, 1393-1402

27. Ono, Y., Hata, S., Sorimachi, H., and Suzuki, K. (2000) *Calcium: The Molecular Basis of Calcium Action in Biology and Medicine*, Kluwer Academic Publishers, Netherlands, 443-464

28. Masumoto, H., Yoshizawa, T., Sorimachi, H., Nishino, T., Ishiura, S. and Suzuki, K. (1998) *J. Biochem.* **124**, 957-961

29. Sorimachi, H., Freiburg, A., Kolmerer, B., Ishiura, S., Stier, G., Gregorio, C. C., Labeit, D., Linke, W. A., Suzuki, K., and Labeit, S. (1997) *J. Mol. Biol.* **270**, 688-695

30. Ishiura, S., Murofushi, H., Suzuki, K. and Imahori, K. (1978) *J. Biochem.* **84**, 225-230

31. Kinbara, K., Ishiura, S., Tomioka, S., Sorimachi, H., Jeong, S. Y., Amano, S., Kawasaki, H., Kolmerer, B., Kimura, S., Labeit, S. and Suzuki, K. (1998) *Biochem. J.* **335,** 589-596

32. Meyer, S. L., Bozyczko-Coyne, D., Mallya, S. K., Spais, C. M., Bihovsky, R., Kaywooya, J. K., Lang, D. M., Scott, R. W. and Siman, R. (1996) *Biochem J.* **314**, 511-519

33. Vilei, E. M., Calderara, S., Anagli, J., Berardi, S., Hitomi, K., Maki, M. and Carafoli, E. (1997) *J. Biol. Chem.* **272**, 25802-2588

34. Rey, M. A. and Davies, P. L. (2002) *FEBS Lett.* **532**, 401-406

35. Labeit, S. and Kolmerer, B. (1995) *Science* **270**, 293-296

36. Porn-Ares, M. I., Samali, A. and Orrenius, S. (1998) *Cell Death Differ.* **5**, 1028-1033

37. Lee, H.-J., Tomioka, S., Kinbara, K., Masumoto, H., Jeong, S.-Y., Sorimachi, H., Ishiura, S. and Suzuki, K. (1999) *Arch. Biochem. Biophys.* **362**, 22-31

38. Nakagawa, K., Masumoto, H., Sorimachi, H. and Suzuki, K. (2001) *J. Biochem.* **130**, 605-611

39. Branca, D., Gugliucci, A., Bano, D., Brini, M. and Carafoli, E. (1999) *Eur. J. Biochem.* **265**, 839-846

40. Fukiage, C., Nakajima, E., Ma, H., Azuma, M. and Shearer, T. R. (2002) *J. Biol. Chem.* **277**, 20678-20685

41. Ma, H., Shih, M., Fukiage, C., Azuma, M., Duncan, M. K., Reed, N. A., Richard, I., Beckmann, J. S. and Shearer, T. R. (2000) *Opht. Vis. Sci.* **41**, 4232-4239

42. Ilian, M. A., Morton, J. D., Bekhit, A. E.-D., Roberts, N., Palmer, B., Sorimachi, H., and Bickerstaffe, R. (2001) *J. Agric. Food Chem.* **49**, 1990-1998

43. Ruiz-Vela, A., González de Buitrag, G., and Martínez-A, C. (1999) *EMBO J*. **18**, 4988-4998

FOOTNOTES

**Present address: Glyco-Chain Functions Laboratory, Frontier Research System, RIKEN, Wako 351-0198, Japan

***Present address: New Frontiers Research Laboratories, Toray Industries Inc., Kamakura 248-8555, Japan

[1]The abbreviations used are: μCL, μ-calpain large subunit; mCL, m-calpain large subunit; p94Δ, p94:exons $6^{-}15^{-}16^{-}$; LGMD2A, limb-girdle muscular dystrophy type 2A; CBB, Coomassie Brilliant Blue; SDS-PAGE, sodium dodecyl sulfate-polyacrylamide gel electrophoresis; PBS, phosphate-buffered saline; 2-ME, 2-mercaptoethanol; BSA, bovine serum albumin; CSTN, calpastatin; ECFP, enhanced cyan fluorescence protein; EYFP, enhanced yellow fluorescence protein; FRET, fluorescence resonance energy transfer.

FIGURE LEGENDS

FIG. 1. Schematic structure of p94:C129S, p94Δ, and purified proteins

(**A**) Schematic structure of p94:C129S and p94Δ. NS, IS1, and IS2 are specific sequences found in p94 but not in the conventional (μ- and m-) calpain large subunits (μCL and mCL). Domains I, III, and V are α-helical, C2-like Ca^{2+}-binding and Gly-rich hydrophobic domains, respectively. Domains IV and VI contains five EF-hand motifs and are very similar to each other. Subdomains IIa and IIb, kept apart in the inactive state, comprise the protease domain when activated. Thick horizontal bars indicate the positions of epitopes for the antibodies used in this study. Note that a part of the epitope for anti-pIS2 is retained in p94Δ. Arrows (1) to (4) indicate the proteolytic sites determined in this study. (**B**) Purified p94:C129S and p94Δ used in this study. Lane 1, molecular weight marker; lanes 2 and 3, p94:C129S (5 μg) and p94Δ (5 μg), respectively, in the final MonoQ fractions (open triangles) were separated electrophoretically and stained with CBB.

FIG. 2. Characterization of p94Δ caseinolytic activity

(**A**) Temperature and incubation-time dependence of activity. Activities were standardized with the value at 37°C for 30 min taken as equal to 1. (**B**) Temperature dependence of activity with 20 min incubation. Closed circles, open lozenges, and open squares represent p94Δ, μ-calpain,

and m-calpain, respectively. Activities were standardized as the maximum value (determined at 42°C for p94Δ, and at 21°C for μ- and m-calpains) equal to 1. (**C**) pH dependence of activity. Activities were standardized with the maximum values equal to 1 (values at pH 7.5 for p94Δ and m-calpain, and at pH 7.4 for μ-calpain). (**D**) Ca^{2+} dependence of activity. Activities were standardized with the maximum value equal to 1 (at pCa = 2.0). (**E**) Activity in the presence of various concentrations of calpastatin (CSTN) domain 1 or related peptides. Sequences of CSTN peptides C9181 and SP007 are given in Fig. 7. Activities were standardized with the value without inhibitor equal to 1. (**F**) The second-phase autolysis of p94Δ in the presence of Ca^{2+}. p94Δ (1 μg) was incubated for 0-90 min on ice or at 30 °C, and visualized by SDS-PAGE and CBB staining. (**G**) Quantification of autolysis fragments of p94Δ. Band intensity of the 84- (full-length, F.L.) and 83- (autolyzed) kDa bands in (**F**) were determined, and plotted after standardizing the value at 0 min as equal to 100%. (**H**) "Intermolecular autolysis" of p94:C129S by p94Δ. p94:C129S (1 μg) and p94Δ (0.1 μg) were co-incubated in the presence of 10 mM $CaCl_2$ for 0-60 min. Samples were subjected to SDS-PAGE, followed by CBB staining, or western blotting using the antibodies indicated. For the positions of the antibody epitopes, see Fig. 1A. The N-terminal sequences of fragments (a)-(d), indicated by triangles, are Ala15, Ala34, Glu323, and Ala34, respectively. These correspond to the proteolytic sites specified by arrows [1], [2], [3], and [2] in Fig. 1, respectively. Arrow heads represent p94Δ

detected by antibody 12A2.

FIG. 3. In vitro *proteolysis of possible substrates of p94Δ*

(**A**) HSP60 degraded proteolytically by p94Δ or m-calpain. HSP60 (0.6 μg) was incubated with 0.3 μg of p94Δ or 0.04 μg of m-calpain in the presence of 10 mM $CaCl_2$ ($+Ca^{2+}$) or 20 mM EDTA (+E) for 0-120 min and visualized by CBB staining. (**B**) Schematic structure of the N2A region of connectin/titin and the binding site for p94. Part of the N2A region of connectin/titin is shown, and the bidirectional arrows indicate the regions corresponding to IgI80-81 and IgI82-83. IgI80-IgI83 are motifs with similarity to immunoglobulin superfamily (I-line region subset); "is" is the intervening region between IgI80 and IgI81; and PEVK is the region rich in Pro, Glu, Val, and Lys. The vertical arrow indicates one of the m-calpain-susceptible proteolytic sites in connectin/titin. CN48 is the original N2A clone isolated by yeast two-hybrid screening using p94 as bait (17), and CN48-Δ1 to -Δ6 were generated from CN48. Each construct was co-transformed with bait plasmid bearing p94 into AH109, and binding was evaluated by growth on SD-LWA plates and β-galactosidase activity (shown in the right column). (**C**) Proteolysis of N2A connectin/titin fragments by p94Δ, μ-calpain, or m-calpain. IgI80-81 (1 μg; upper) or IgI82-83 (1 μg; lower) connectin/titin N2A recombinant peptide was incubated with 2, 1, 0.5, 0.2, or 0.1 μg (left to right in each panel) of p94Δ (left), m-calpain (middle), or μ-calpain (right) in the

presence of 15 mM $CaCl_2$ for 60 min at 37 °C for p94Δ, or for 20 min at 30 °C for m- and μ-calpains. The lanes labelled "+E" contain 2 μg of p94Δ (left), m-calpain (middle), or μ-calpain (right) incubated with each peptide in the presence of 20 mM EDTA where no autolytic degradation occurred. Closed triangles indicate p94Δ, mCL, or μCL and open triangles indicate uncleaved connectin/titin peptide, IgI80-81 or IgI82-83. Protein fragments were visualized by CBB staining. (**D**) m-calpain:C105S degraded proteolytically by p94Δ. p94Δ (2 μg) and m-calpain:C105S (1.5 μg) were co-incubated for 0-120 min in the presence of 15 mM $CaCl_2$, 20 mM EDTA (+E), or 15 mM $CaCl_2$ and 0.7 μg of calpastatin domain 1 (+CSTN). Samples were subjected to SDS-PAGE, and proteins detected by CBB staining or western blotting using anti-human m-calpain or anti-pIS2 antisera.

FIG. 4. Proteolysis of calpastatin by p94Δ

(**A**) Processes of calpastatin proteolysis by p94Δ determined by reversed-phase column chromatography. Calpastatin domain 1 (30 μg) and p94Δ (1 μg) were co-incubated in the presence of 15 mM $CaCl_2$ for 0-120 min at 37 °C. The reaction was stopped at each time point by adding 1 ml of 0.1% TFA, and the products were subjected to C18 reversed-phase column chromatography (RPC) with a 10-50% acetonitrile gradient. Closed triangles in the 20 min digestion represent fractions of peptides degraded at the most susceptible sites in calpastatin,

judged by the earliest appearance of these peaks. Lower-case letters on open triangles in the 60 min digestion correspond to the fractions in (B). (**B**) Tris-tricine gel electrophoretic analysis of proteolytic fragments of calpastatin (digested for 60 min). Lower-case letters on the top of the panel correspond to fractions labelled in (A). T and U stand for total protein before separation by RPC, and undigested calpastatin domain 1, respectively. (**C**) Comparison of sites of calpastatin cleavage by p94Δ. All six N-terminal sequences identified from the digestion of calpastatin domain 1 (i-vi) and one from the digestion of calpastatin peptide C9181 (vii) are shown. The autolytic sites at the N-terminus (N-1 and -2) and in the IS1 region (IS1-1 to -3) are also shown for comparison (31). The vertical arrow indicates the proteolytic site. Proline residues are reversed. (**D**) Alignment of human and rabbit calpastatin inhibitory domains 1-4 and positions of the proteolytic sites for p94Δ. Amino acid sequences around the inhibitory reactive site (indicated by the bidirectional arrow) are shown, and highly and moderately conserved residues are reversed and shaded, respectively. The open triangle indicates the position of the caspase proteolytic site (36). Thick lines indicate the sequence corresponding to the commercially available calpastatin peptides, C9181 and SP007, used in this study. Vertical arrows with numbers correspond to the sequence labels in (**C**).

FIG. 5. Assay for p94Δ utilizing calpastatin and FRET of fluorescence proteins

(**A**) Schematic structure of p94Δ-specific substrate (Y-C-CSTN) used in this study. CSTN represents residues 157-255 of rabbit calpastatin (GenBank/EMBL/DDBJ accession number A26615). (**B**) Steps in substrate processing by p94Δ. Y-C-CSTN (2 μg) was incubated alone (-p94Δ) or with 1.5 μg of p94Δ (+p94Δ) in a buffer composed of 15 mM Ca^{2+}, 1 mg/ml BSA, 0.1 mg/ml CSTN, 10 mM 2-ME, and 100 mM Tris-Cl (pH 7.5) in a volume of 15 μl for 0-45 min at 37 °C. CBB staining. (**C**) Changes in the fluorescence spectrum of the substrate during proteolytic digestion by p94Δ. Reactions in (B) (+p94Δ) were terminated by the addition of 0.5 ml of 50 mM EDTA (pH 8.0) and the fluorescence emission spectra from 450 to 600 nm excited by 434 nm were scanned. (**D**) Dose-dependent fluorescent signals in this assay system. p94Δ (0-2 μg) was incubated with 0.6 μg of Y-C-CSTN under the same conditions as in (B), but in the presence of 28 mM Ca^{2+}. Reactions were stopped by adding 0.5 ml of 50 mM EDTA (pH 8.0), and the fluorescence emission of 476 nm and 527 nm excited by 434 nm light was measured. The ratio of fluorescence at 477 nm to that at 527 nm was plotted. (**E**) Activity of COS-expressed full-length wild-type p94 and p94Δ. The lysate from COS-7 cells (2.5×10^5) transfected with either the pSRD vector, or vectors expressing full-length wild-type p94 (f.l.p94), p94Δ, full-length p94:C129S (CS), or μ-calpain (μ-calpain) was prepared by sonicating the cells in 50 mM Tris-Cl (pH 7.5) buffer supplemented with 25 mM 2-ME, 10 mM EDTA, and the

following protease inhibitors: 10 μM Z-D-CH2-DCB, 10 μM YVAD-CMK, 1 mM AEBSF, 2 μM calpastatin peptide C9181, and 2 mM PMSF. The lysate was incubated with Y-C-CSTN in the presence of 5 mM Ca^{2+} (+) or 10 mM EDTA (-) at 37 °C for 90 min. Measurements and calculations were as in (D). The values shown are representative of three independent experiments and are averages calculated using duplicate measurements. (**F**) Autolysis of COS-expressed p94 simultaneous with substrate hydrolysis. Reactions were carried out essentially as in (E) except that they were stopped by the addition of half a volume of 3 × SDS sample buffer. Western blot analysis of p94 (f.l.p94), p94Δ, and full-length p94:C129S (CS) with the antibody 12A2 and of μ-calpain (μ-calpain) with the antibody MAB3082 showed Ca^{2+}-independent and Ca^{2+}-dependent autolysis only for p94 and p94Δ, respectively.

Table 1 Effects of various protease inhibitors on p94Δ, μ- and m-calpain

Values are relative to the inhibitory activity of 0 and 10 mM EDTA, which are set to 0 and 100, respectively.

Name	conc.	p94Δ	μ-calpain	m-calpain
EDTA	10 mM	**100**	**100**	**100**
Leupeptin	1 mM	102	101	100
	0.1 mM	86.7	98.7	97.8
E-64c	0.1 mM	101	101	76.6
	10 μM	87.0	91.2	90.7
Chymostatin	1 mM	85.1	90.7	84.1
Calpeptin (ZLNal)	10 μM	76.1	98.7	98.1
	1 μM	19.0	88.9	87.6
TPCK	1 mM	65.2	57.4	73.1
ALLNal (MG-101, calpain inhibitor I)	10 μM	64.1	90.1	88.7
MG-132 (ZLLLal)	1 μM	14.9	35.9	56.6
PD150606	10 μM	11.7	55.0	73.4
	1 μM	6.52	14.3	44.5
Calpastatin domain 1	0.14 μM	4.36	77.2	76.1
Pepstatin A	10 μM	3.26	1.44	3.85
AEBSF	10 mM	0	0	0
Aprotinin	15 μM	0	0	0
Bestatin	1 μM	0	0.160	0
1-10-Phenanthrolin	20 mM	0	0	0
Phosphoramidon	0.1 mM	0	0	0
PMSF	10 mM	0	0	0
TLCK	1 mM	0	0	7.97

Ono, Y. et al., Fig. 1

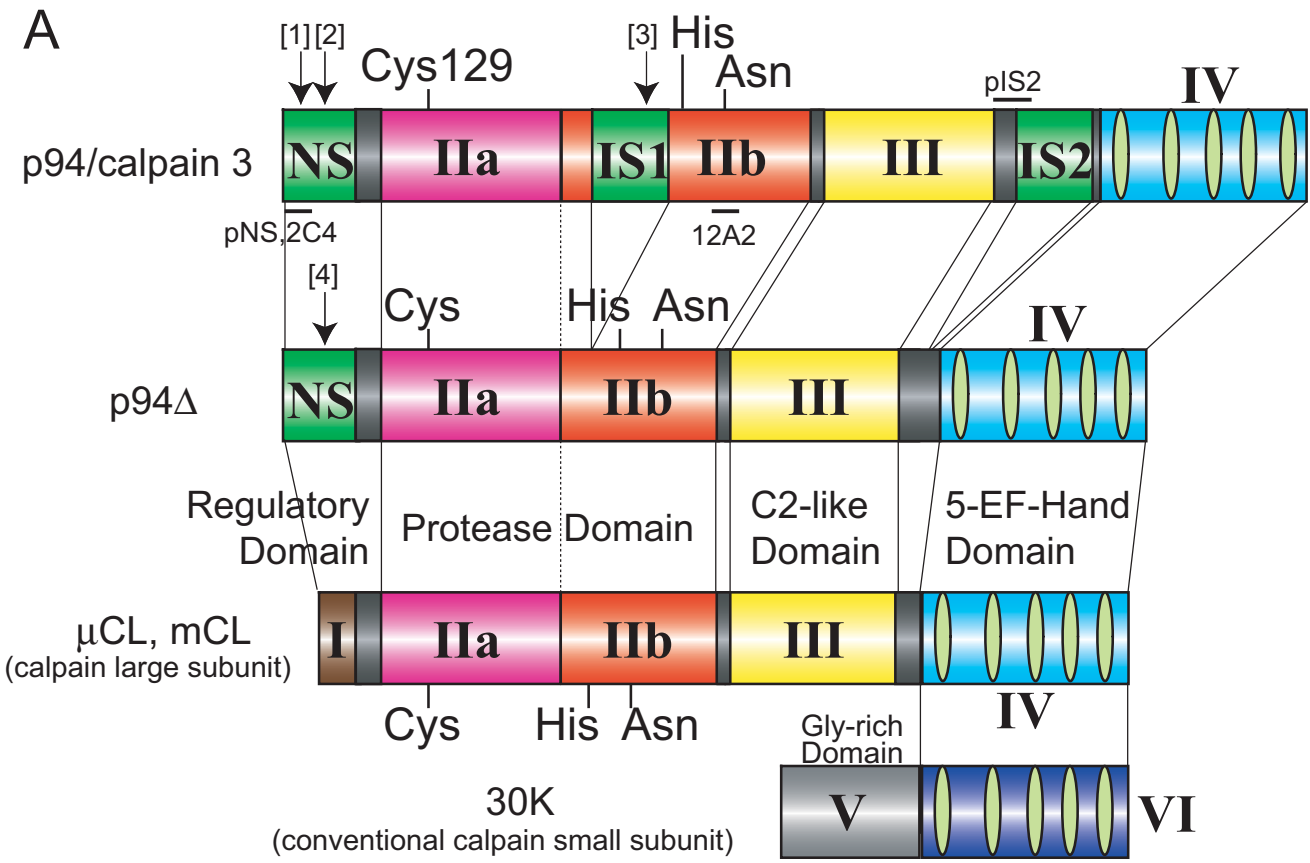

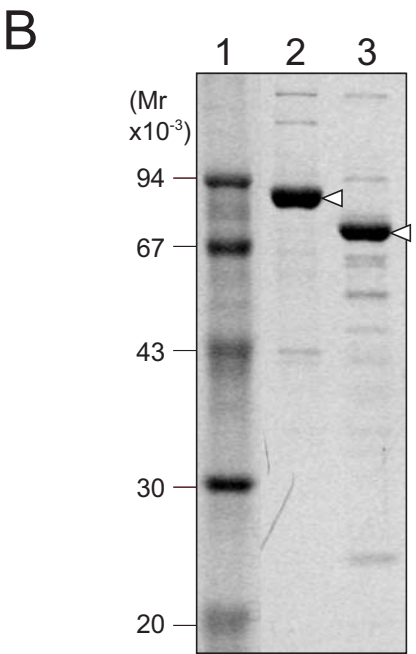

Ono, Y. et al., Fig. 2

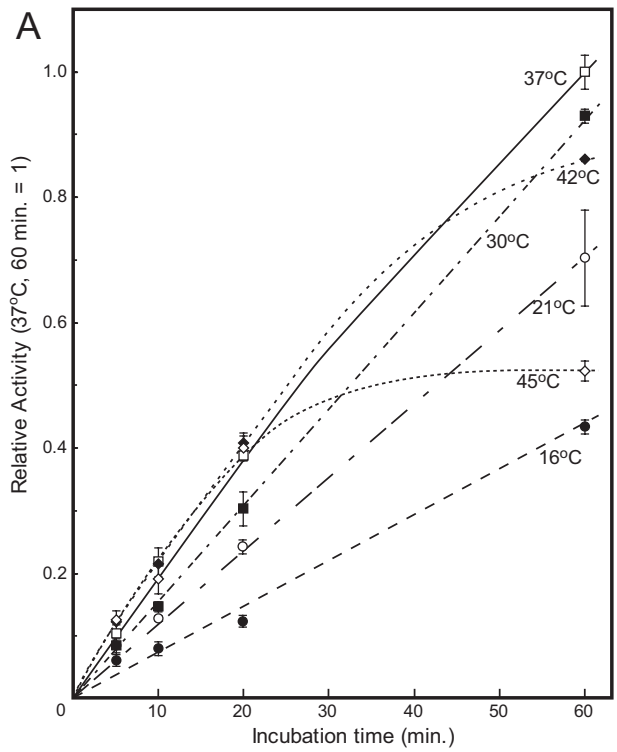

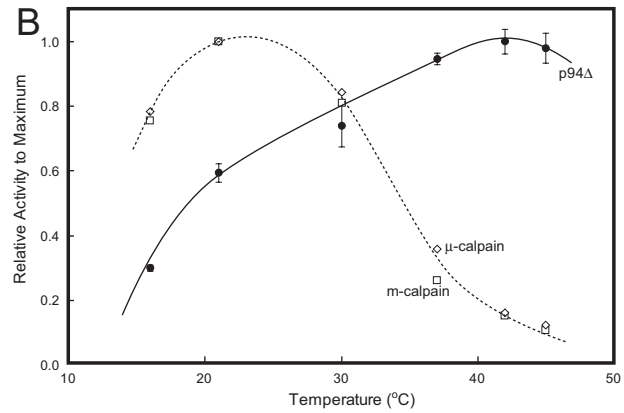

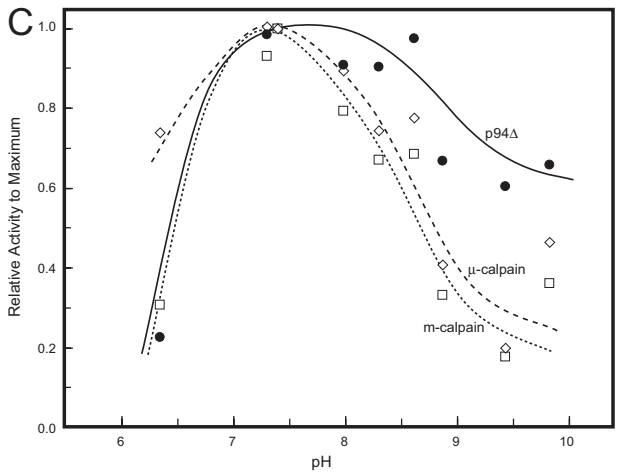

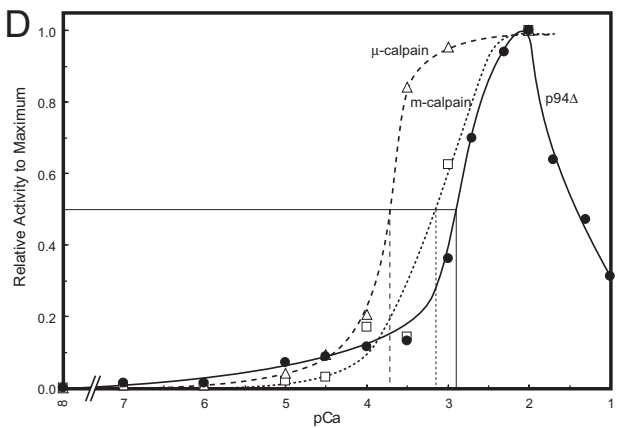

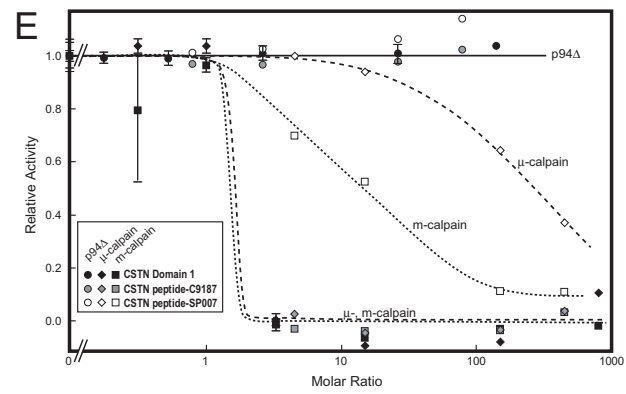

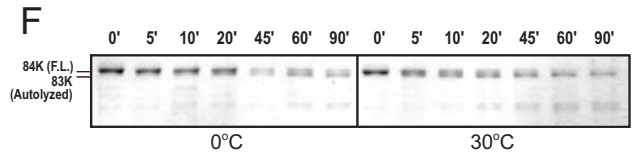

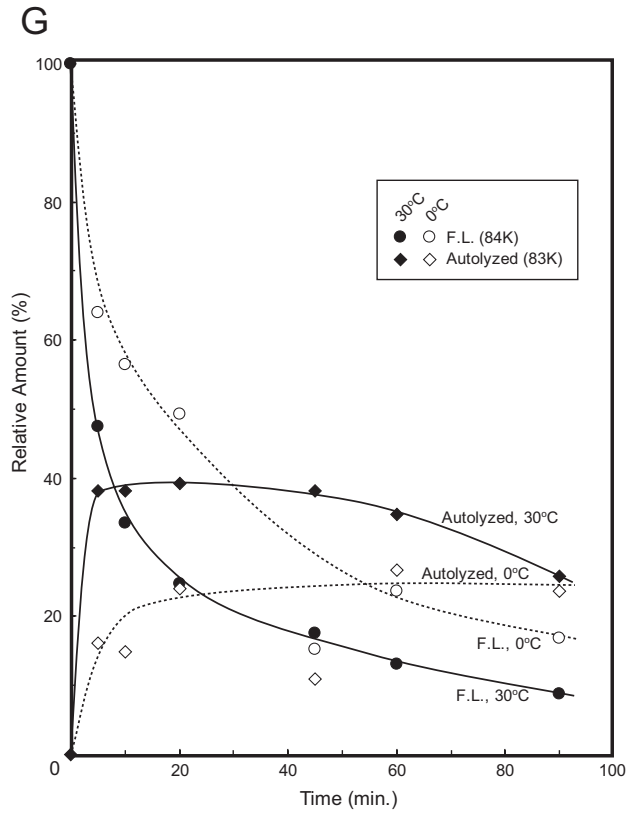

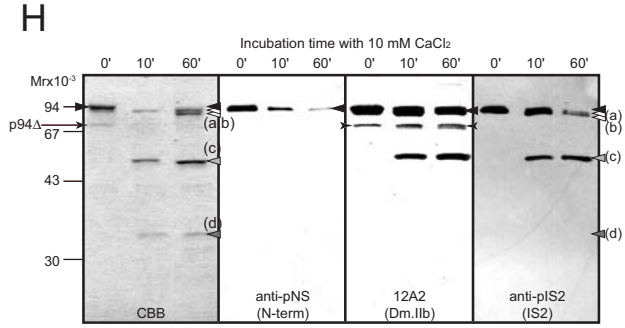

Ono, Y. et al., Fig. 3

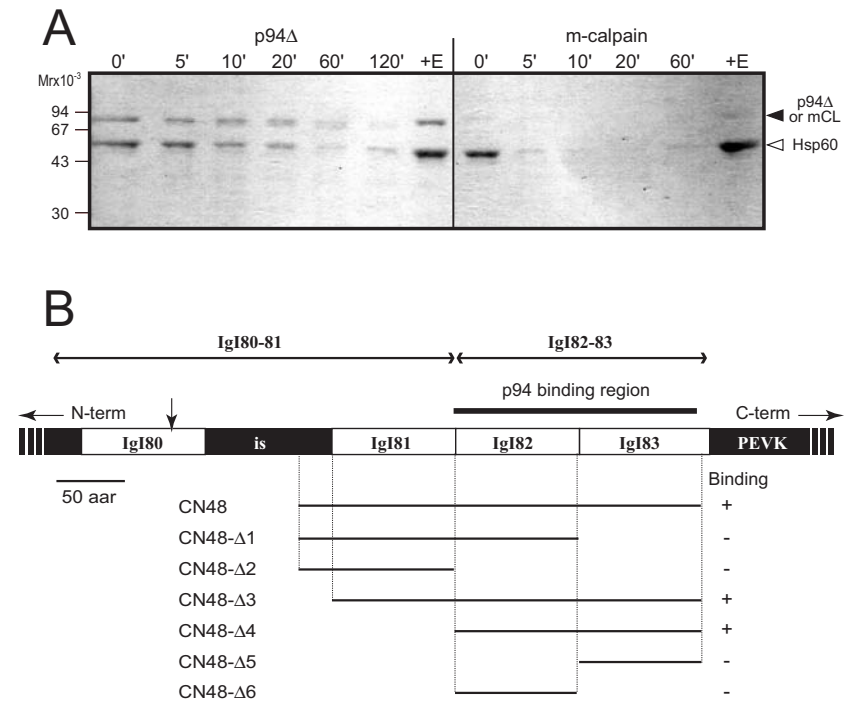

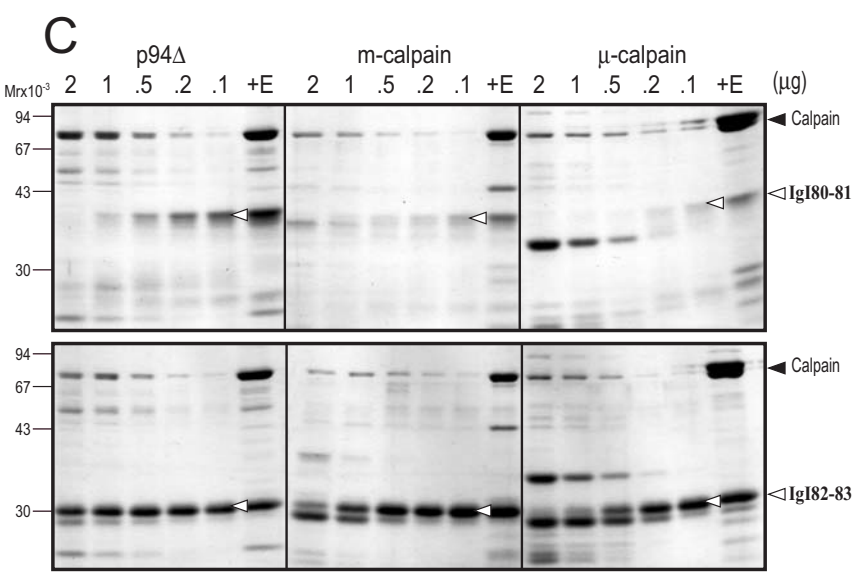

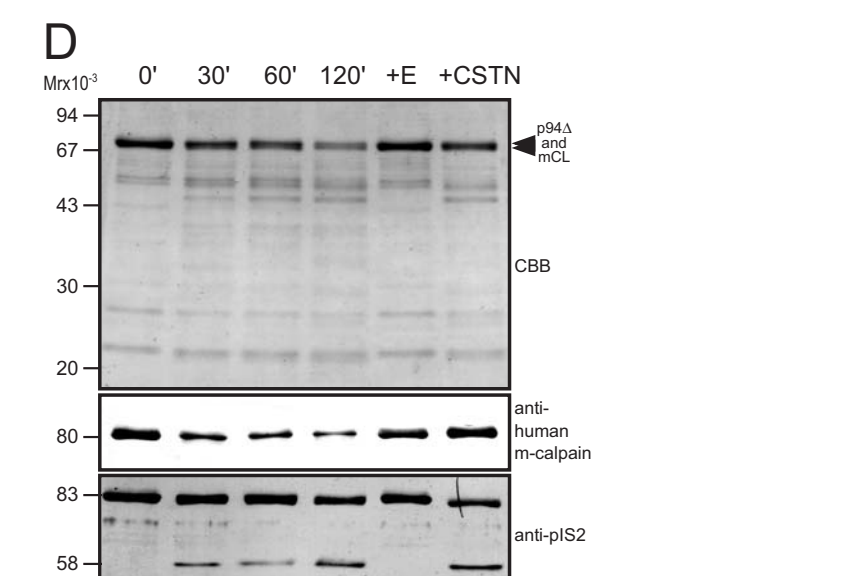

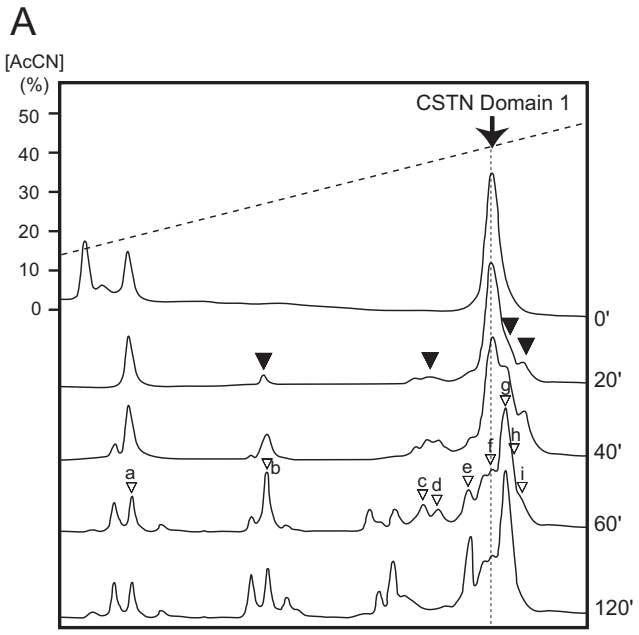

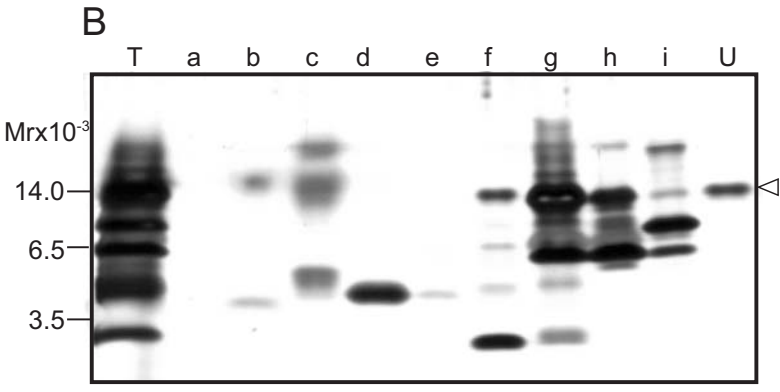

C

		8	7	6	5	4	3	2	1	1'	2'	3'	4'	5'	6'	7'	8'
i.	83	S	T	Y	I	E	E	L	G	K	R	E	V	T	I	P	P
ii.	97	P	P	K	Y	R	E	L	L	A	K	P	I	G	P	D	D
iii.	98	P	K	Y	R	E	L	L	A	K	P	I	G	P	D	D	A
iv.	116	A	L	S	S	D	F	T	C	G	S	P	T	A	A	G	K
v.	141	V	L	K	A	Q	S	A	G	T	V	R	S	A	A	P	P
vi.	144	A	Q	S	A	G	T	V	R	S	A	A	P	P	Q	E	K
vii.	91	K	R	E	V	T	I	P	P	K	Y	R	E	L	L	A	K
N-1	2	A	S	V	A	P	R	T	A	A	E	P	R	S	P	G	P
N-2	26	P	A	Q	S	K	A	T	E	A	G	G	G	N	P	S	G
IS1-1	267	D	D	G	T	N	M	T	Y	G	T	S	P	S	G	L	N
IS1-2	289	R	M	V	R	N	M	D	N	S	L	L	Q	D	S	D	L
IS1-3	315	R	T	I	I	P	V	Q	Y	E	T	R	M	A	C	G	L

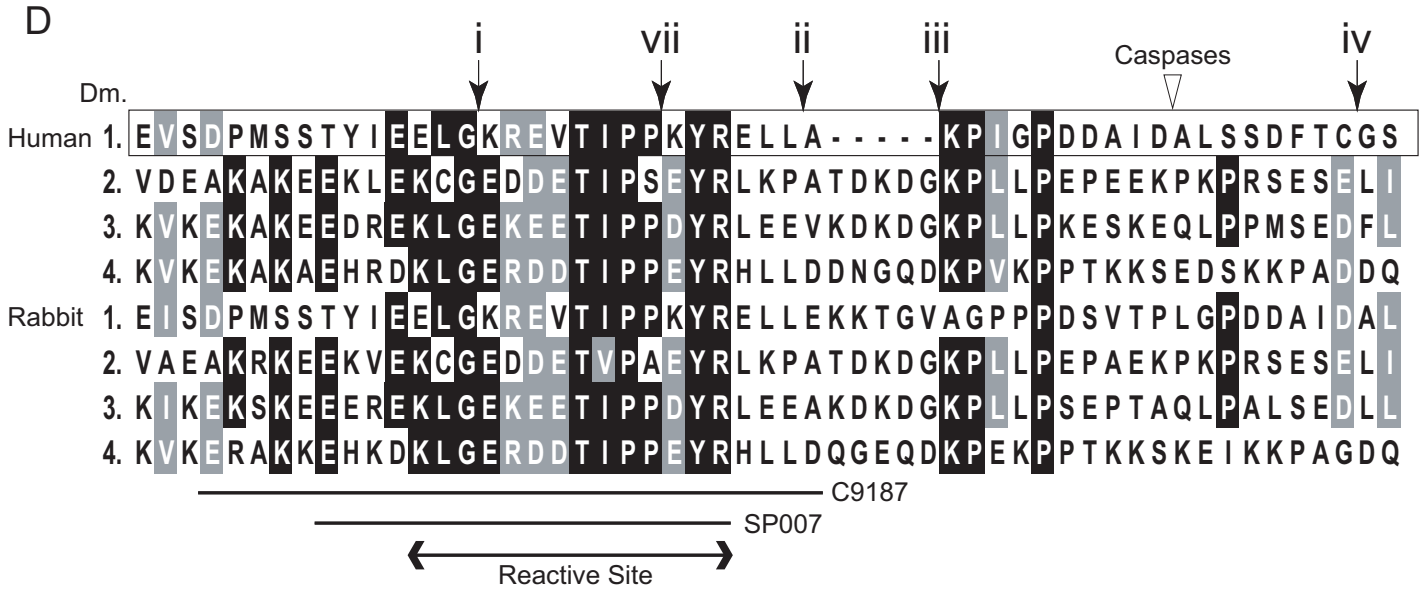

Ono, Y. et al., Fig. 5